POLAR PLASMAS AS OBSERVED BY DYNAMICS EXPLORERS 1 AND 2*

J. Barfield, J. Burch, C. Gurgiolo, C. Lin, D. Winningham, and N. Saflekos
Southwest Research Institute
San Antonio, Texas 78284

Plasma measurements from the Dynamics Explorer 1 and 2 satellites have been used to characterize the polar cap environment. Analysis of numerous polar-cap passes have indicated that, in general, three major regimes of plasma exist:

(1) polar rain--electrons with magnetosheath-like energy spectra but much lower densities, most intense near the cusp and weakening toward the central polar cap;

(2) polar wind--low energy upward flowing ions with both field-aligned and conical distributions;

(3) acceleration events--sporadic events consistent with the acceleration of electrons and positive ions by parallel electric fields.

(1)-(3) have been observed at high altitudes by Dynamics Explorer 1, while (1) and (3) have been observed at low altitudes by Dynamics Explorer 2. The plasma parameters associated with these plasma regimes are presented and discussed in terms of source and acceleration mechanisms.

INTRODUCTION

The polar cap is a region threaded by magnetic field lines which intersect the earth poleward of the auroral oval. The magnetic field lines of the polar cap are generally accepted as either being open or closed at such large distances from the earth that they are effectively open. This linkage between the polar cap ionosphere and the interplanetary medium makes the polar caps extremely important in the study of the interaction between the solar wind and the high-latitude ionosphere. Since the polar caps are not directly connected to those closed-line regions of the magnetosphere where plasma and energy are stored, electric fields, currents, and particle precipitation in the polar caps respond quickly to changes in solar wind conditions. Many authors have studied the relationships between the solar wind conditions and the polar-cap environment. However, much remains unknown at present concerning the characteristics of polar cap plasmas.

*This work was supported by the Air Force Geophysics Laboratory under Contracts F19628-82K-0024 and FY7121-83-N-001, by NASA under Contracts NAS5-26363 and NAS5-25693, and by the Southwest Research Institute Internal Research Program.

Examination of the DE-1 and DE-2 data has provided new information on three major polar-cap plasma regimes:

(1) polar rain--electrons with magnetosheath-like energy spectra but much lower densities, most intense near the cusp and weakening toward the central polar cap;

(2) accelerated polar wind--low energy upward flowing ions with both field-aligned and conical distributions;

(3) acceleration events--sporadic events consistent with the acceleration of electrons and positive ions by parallel electric fields.

The Dynamics Explorer satellites, launched in 1981, have afforded new and unique opportunities to probe polar cap plasmas. (Details of the satellites, their orbits, and instrumentation may be found in Space Science Instrumentation, Vol. 5, No. 4, 1981--special issue.) The combined high-altitude polar orbit of Dynamics Explorer 1 (DE-1) and the low-altitude polar orbit of Dynamics Explorer 2 (DE-2) have been used to observe the polar cap plasma environment on a large number of passes.

The next section briefly describes the instrumentation used for the observations. Following that, the next three sections present observations.

INSTRUMENTATION

The DE-1 satellite was launched on August 3, 1981, into an elliptical polar orbit with an apogee of 4.6 R_E geocentric and a perigee of 650 km altitude. The DE-1 High Altitude Plasma Instrument (HAPI) consists of five electrostatic analyzers mounted in a fan-shaped angular array at angles of 45°, 78°, 90°, 102°, and 135° with respect to the spacecraft spin axis. Each analyzer makes differential measurements of positive ions and electrons over an energy per charge range of 5 eV/e to 32 keV/e. The energy stepping rate may be commanded over a range up to 64 sec^{-1}, producing three-dimensional plasma distributions at the six-second spin period of DE-1 (see ref. 1 for details).

The DE-2 satellite, launched with DE-1 on August 3, 1981, has an elliptical polar orbit at approximately 300 x 1000 km altitude. DE-2 is three-axis stabilized, with one axis in the zenith, another perpendicular to the orbit plane, and the last completing a right-hand triad. The DE-2 Low Altitude Plasma Instrument (LAPI) consists of 15 ion and 15 electron energy/unit charge analyzers mounted on an external scan platform (ref. 2). The detector array can be held approximately fixed (<1°) with respect to the local magnetic field vector. The plane of the sensors is in the orbital plane and thus in the local magnetic meridian plane. Two pairs of out-of-plane detectors allow for sampling near 0° and 180° pitch-angle when the magnetic field vector deviates significantly from the plane of the detector array.

OBSERVATIONS

Polar Rain

Winningham and Heikkila (ref. 3) first described polar rain, using data from the

ISIS 1 satellite. Polar rain is the most common type of particle precipitation over the polar caps. This broad and relatively structureless electron precipitation can often fill the entire polar cap. The precipitating electrons typically have thermal energies on the order of 100 eV and are isotropic over the downcoming hemisphere. The energy flux carried by the particles is of the order of 10^{-3} to 10^{-2} erg $cm^{-2}sec^{-1}$ (ref. 4). The spectral distribution of the polar rain electrons has the same shape as that of cusp electrons, but is lower in intensity, suggesting that polar rain originates in the magnetosheath and travels to the polar ionosphere via the lobes of the magnetotail.

Figures 1a and 1b show differential energy flux from the LAPI instrument aboard DE-2 for a portion of a polar pass on day 295 (22 October) of 1981. The top panel shows data for 8° pitch angle electrons, and the bottom panel shows 45° pitch angle ion data. The upper center panel shows 90° and 0° pitch angle electron data from the GM tube. The data are coded according to the color bars at the right. Satellite ephemeris is shown at the bottom. In this particular pass, DE-2 passed through the northern polar cusp at approximately 1306-1307 UT and into the polar cap. The polar rain can be seen clearly as a bright band in the electron panel over the energy range ≈60-600 eV. The electron flux intensity remained fairly constant in intensity until just after 1309 UT when it abruptly decreased. Notice the lack of ion fluxes over the polar cap.

Figure 2 shows line plots of the average energy, energy flux, and density of the downcoming electrons for 1306-1311 UT. These parameters are obtained by integrating distribution functions over energy from 5 eV to 20 keV. During the entire interval, the average electron energy and density remained roughly constant. The average energy was about 100 eV and the density of downcoming electrons was in the range of 1-5 cm^{-3}. These values of energy and density are representative of the polar rain. After exit from the cusp at about 1307 UT, the energy flux increased very slightly toward the pole until just after 1309 UT when it decreased by approximately 50%.

Figure 3 shows a DE-1 high-altitude polar pass approximately three hours after the DE-2 pass shown in Figure 1. During the interval 1617-1619 UT, DE-1 traversed the magnetic local time and invariant latitude corresponding to those of DE-2 just poleward of the cusp in Figure 1a. The format is the same as for Figure 1, except for the absence of GM tube data. The polar rain may be seen as a band in the spectrogram over the energy range ≈100-600 eV. Bracketing the polar rain are counterstreaming energetic (E>600 eV) electron beams at 0° and 180° pitch angle and upward-moving low-energy (E<100 eV) electron beams. The source of the energetic counterstreaming electrons is open to question and presently under study by Gurgiolo and Burch (unpublished). Two possibilities for the source would be reflection by a potential barrier at the magnetopause (ref. 6) or direct access of solar electrons. Upstreaming ion conics may be seen in the lower panel.

Comparing Figure 1 and Figure 3, it is interesting to note that the polar rain is of the same spectral nature at both altitudes, suggesting the absence of any significant acceleration between the two satellite locations. To demonstrate further the similarity between the electrons at the two satellites, Figure 4 shows number density, energy flux, and average energy at DE-1 for the period 1614-1619 UT. The average energy was ≈100 eV, density was ≈1 cm^{-3} and the energy flux was 0.8 ergs $cm^{-2}s^{-1}$. The corresponding values at lower altitudes were ≈100 eV, ≈2 cm^{-3}, and ≈0.8 ergs $cm^{-2}s^{-1}$.

A detailed look at the near-field-aligned electron populations at the two satellite locations is provided in Figure 5. Shown are three data sets - two single energy sweeps from LAPI, one just at the poleward edge of the cusp and one approximately 10° poleward of the cusp, and a single energy sweep from HAPI at a location which maps to near the location of the first LAPI spectrum. From Figure 3, we first can see that above photoelectron energies the LAPI population can be represented by a Maxwellian, allowing the temperatures to be estimated. Near the cusp a least squares fit gives a temperature of 92 eV, while farther poleward the temperature is 99 eV. The HAPI spectrum appears well-fitted by two Maxwellians above photoelectron energies. The low-energy population has a least-squares fit temperature of 65 eV, while the higher energy population has a temperature of 141 eV.

Accelerated Polar Wind

The polar wind refers to the continual escape of ionospheric plasma from the polar ionosphere along open magnetic field lines. This escape of particles has consistently been observed to lead to a depletion of light ionospheric ions (ref. 7) and electrons in the upper polar ionosphere. Until recently, observations of the polar wind in the literature were limited to the low-altitude observations of Hoffman and Dodson (ref. 7). They reported a continual upward flow of H^+ and He^+ over the polar caps in the range 1-5 km/sec and 1-3 km/sec, respectively. The low energy of these particles precluded most instruments from directly obtaining a distribution function. However, as pointed out by Gurgiolo and Burch (ref. 5), polar-wind models predict that the particle velocity should increase with altitude (ref. 8). Thus, the high altitude satellite DE-1 is an ideal platform from which to study the polar wind.

Plasma data from DE-1 polar passes indicate that ions with peak differential energy fluxes in the 5 to 100 eV range are continually flowing out of the dayside cusp and polar cap. The flows have both a field-aligned and a conic component. The field-aligned component is unmistakably the polar wind. Gurgiolo and Burch (ref. 5) concluded that the conics observed in conjunction with the polar wind are polar-wind ions that have been perpendicularly heated.

The polar-wind observations to be discussed were made during a polar pass on day 272 (September 29) of 1981. Figure 6 consists of 3 sets of particle spectrograms on the same format as Figure 3. Each spectrogram displays the differential energy flux for the particle detectors which lie closest to the plane containing the local magnetic field vector.

Figure 6 shows a continuous band of upward flowing ions (near 180° pitch angle). The satellite was inside the cusp during the interval covered in Figure 6a. At 1411 UT, the satellite passed through the poleward cusp boundary. The upward ions showed a gradual increase in energy throughout and slightly poleward of the cusp, then they begin to decrease steadily, the peak in the differential energy flux eventually dropping below the lowest energy channel of HAPI. Within the cusp, the conic and field-aligned ions appear as "tuning forks" in the spectrograms. In the polar cap the conics become less and less apparent, as the energy and angular separation of the conic and field-aligned ions decrease. In the polar cap, there also is a shift in the field-aligned ions from ≈180° pitch angle to ≈165°, indicating an antisunward flow.

Figure 7 shows a detailed view of the field aligned ion population. Two data sets are shown, each of which was averaged over four satellite revolutions to improve counting statistics. Each of the distributions was transformed to the rest frame of

the plasma prior to averaging (except for S/C charging which was about 20V). The two data sets were taken beginning 1434:05 UT (solid circles) and 1434:54 UT (open circles). In Figure 7 Maxwellian distributions are straight lines, with the slope being proportional to the plasma temperature and the intercept with the distribution axis being proportional to the plasma density.

From Figure 7 we can see that the field-aligned ion component observed in the polar regions is comprised of two ion populations--a low energy component with temperature below .5 eV and a high energy tail with temperature above 1.5 eV. Both ion populations would appear to be well represented by a Maxwellian distribution, allowing the estimates of the temperatures to be made. A least squares fit to the low-energy population of Figure 7 gives a temperature of .29±.16 eV (3200°K±1800K). The corresponding temperature of the high energy plasma population in Figure 7 is found to be 2.7±.7 eV. The peak at about 1 eV may be due to an ion heavier than H^+.

There is little doubt that the lower energy, field-aligned ions constitute the "classical" polar wind. The high energy tail, however, is not a feature predicted by polar-wind models. It is likely that this hotter plasma is the result of a perpendicular heating of polar-wind ions. Assuming that all ions in the polar wind are of equal temperature, Figure 7 gives heating on the order of 4 to 10.

We envision a scenario as shown in Figure 8 occurring during the polar wind escape along magnetic field lines. At low altitudes the generation of the polar wind occurs and ionospheric ions begin to escape along the open polar cap and cusp field lines (Figure 8a). The presence of ion perpendicular heating along the open field lines produces the characteristic conic signature (Figure 8b). The distribution above the heating region can be considered a two-component plasma consisting of unheated and heated polar-wind particles. The unheated polar wind is still field aligned, while the heated ions have large velocities in the direction perpendicular to $\underline{B}$. As the distribution travels upward, the perpendicular arms of the distribution will begin to collapse toward the magnetic field direction in accordance with the first adiabatic invariant, and a field-aligned high energy tail to the polar wind should develop (Figure 8c). Figure 8d shows contours of a typical conic/polar-wind population measured in the cusp on day 272.

Ion conics have been reported by numerous people (Refs. 9 and 10). Theories as to the production of the conic ion distribution have favored a perpendicular heating by electrostatic ion-cyclotron waves (ref. 9, refs. 11 and 12), although recently (ref. 13) it has been proposed that a heating by lower hybrid waves may also be a viable conic generation mechanism. The problem is, however, that most of these theories are applicable only at low altitudes in the auroral zone. Adaptations of the theories to the environment of the polar cap must be made to explain these observations.

Using the observed conic pitch angle distribution, the altitude of the observation and an assumed value for the initial conic pitch angle, it is possible through the first adiabatic invariant to estimate the altitude of the conic generation. In general the initial conic pitch angle for such computations is assumed to be 90°; however, if the source plasma already has a significant $V_{\parallel}$, as the polar wind does, then the initial conic pitch angle is expected to shift to lower values. Using a dipolar magnetic field approximation and estimating the values of the initial conic pitch angle through energy conservation arguments (which assume that $V_{\parallel}$ does not

change between the observation height and the conic height) we estimate the heating to occur at an altitude of about 12,000 km--constant throughout both the cusp and polar cap. By using an initial conic pitch angle of 90° we can place a lower limit to the heating altitude at 8000 km.

Acceleration Events

The electrical coupling between the high-altitude and low-altitude regimes of the polar cap is an important aspect of magnetosphere-ionosphere interactions. The unique placement of the Dynamics Explorer orbits with respect to each other has afforded an excellent opportunity to investigate this coupling between the two regimes. Frequently, DE-1 and DE-2 observe signatures of field-aligned acceleration of ions and electrons above the polar cap. In this section, we briefly present observations made on October 17, 1981 (day 81290) above a "theta aurora" signature.

Figure 9 shows a spectrogram of 180° ions and 0° pitch angle electrons from HAPI. The satellite crossed the polar-cap arc field lines during the interval 1630-1650 UT. Two intervals of intense electron fluxes below 1 keV were seen: ≈1631:30-1633:15 UT and ≈1642-1649 UT. Figure 10 shows contour plots of the log of the distribution functions of ions (Figure 10a) and electrons (Figure 10b) for the interval 1632:45-1632:57 UT. The ions showed a strong upgoing beam at approximately 100 eV. The electron fluxes were isotropic except for a loss cone. Thus, the combined electron and ion observations indicated that an approximately 100 eV potential drop lay below the satellite altitude.

Figure 11 shows contours in the same format as Figure 10, for the interval 1646:30 to 1646:36 UT. By this time the ions had become isotropic, while the electrons showed a downcoming beam of ≈100 eV. Thus, the acceleration region appears now to be above the satellite altitude (17313 km) while remaining at ≈100 eV.

The plasma characteristics described above are very similar to those observed by DE-1 in the high altitude (>15,000 km) nightside auroral zone, except that the energy of the polar cap acceleration events is lower. Correlation studies by Hardy et al. (ref. 14) have already noted that the plasma signatures of polar cap acceleration events at low altitudes are similar to those of evening discrete arcs. The parallel electric field responsible for the polar-cap acceleration could be produced by the same process as the evening auroral arcs.

Satellite observations of convection and electron precipitation at low altitudes (<1000 km) have indicated that convective electric fields point toward the region of polar-cap acceleration ($\nabla \cdot E < 0$) (ref. 15). The polar cap acceleration region is therefore a region of negative space charge. Burke et al. (ref. 16) used the simultaneous electric field, magnetic field and electron flux measurements of the S3-2 satellite to demonstrate that upward Birkeland currents were embedded in regions of polar cap acceleration. These observations suggest that field-aligned potentials develop as a result of imperfect mapping of magnetospheric convective electric fields to the ionosphere (ref. 14; ref. 16).

SUMMARY AND CONCLUSIONS

Plasma measurements made on the Dynamics Explorer 1 and 2 spacecraft are providing new information on the altitude dependence of polar-cap plasma populations, their sources, and the acceleration processes they undergo. In this study we have found that the polar-rain electron population apparently exhibits no significant altitude dependence between altitudes of a few hundred to ~20,000 km. This result was expected from the magnetosheath-like energy spectrum of the low-altitude polar rain.

In the case of the polar wind, a significant velocity increase was theoretically predicted to occur between the two spacecraft altitudes, and this effect has been confirmed by the DE-1 plasma measurements. A major result of our study of the accelerated polar wind is its significant conic component, which indicates that the ions are heated perpendicularly as they emerge from the polar-cap ionosphere. The gradual decrease in polar-wind energy that is observed to occur from the cusp across to the nightside polar cap suggests that the perpendicular heating process, probably in cyclotron waves, is most intense near the cusp region.

Significant altitude effects are also observed in the plasmas that occupy magnetic flux tubes connected to polar-cap auroral arcs (or theta auroras). At DE-2, typical low-energy (~100 eV) inverted-V electron distributions are observed. At DE-1 the electron and positive-ion distribution functions are consistent with electrostatic potential drops that are at times below the typical DE-1 altitude of 15,000 to 20,000 km and at times above these altitudes. Thus, compared to auroral-oval acceleration regions those in the polar cap appear to be weaker and at significantly higher altitudes.

REFERENCES

1. Burch, J. L., J. D. Winningham, V. A. Blevins, N. Eaker, W. C. Gibson, and R. A. Hoffman: High-Altitude Plasma Instrument for Dynamics Explorer-A, Space Sci. Instr., 5, 455, 1981.

2. Winningham, J. D., J. L. Burch, N. Eaker, V. A. Blevins, and R. A. Hoffman: The Low Altitude Plasma Instrument (LAPI), Space Sci. Instr., 5, 465, 1981.

3. Winningham, J. D. and W. J. Heikkila: Polar Cap Electron Fluxes Observed with ISIS-1, J. Geophys. Res. 79, 949, 1974.

4. Burke, W. J.: Magnetosphere-Ionosphere Coupling: Contributions from IMS Satellite Observations, Rev. Geophys. Space Phys., 20, 685, 1982.

5. Gurgiolo, C. and J. L. Burch: DE-1 Observations of the Polar Wind--A Heated and an Unheated Component, Geophys. Res. Lett. 9, 945, 1982.

6. Foster, J. C. and J. R. Burrows: Electron Fluxes over the Polar Cap 1. Intense keV Fluxes During Poststorm Quieting, J. Geophys. Res., 81, 6016, 1976.

7. Hoffman, J. H. and W. H. Dodson: Light Ion Concentrations and Fluxes in the Polar Regions during Magnetically Quiet Times, J. Geophys. Res., 85, 626, 1980.

8. Schunk, R. D. and D. S. Watkins: Proton Temperature Anisotropy in the Polar Wind, J. Geophys. Res., 87, 171, 1982.

9. Ungstrup, E., D. M. Klumpar, and W. J. Heikkila: Heating of Ions to Superthermal Energies in the Topside Ionosphere by Electrostatic Ion Cyclotron Waves, J. Geophys. Res., 84, 4289, 1979.

10. Gorney, D. J., A. Clarke, D. R. Croley, J. F. Fennell, J. Luhman, and P. Mizera, The Distributions of Ion Beams and Conics below 8000 km, J. Geophys. Res., 86, 83, 1981.

11. Dusenbery, P. B., and L. R. Lyons, Generation of Ion-Conic Distribution by Upgoing Ionospheric Electrons, J. Geophys. Res., 86, 7627, 1981.

12. Lysak, R. L., M. K. Hudson and M. Temerin: Ion Heating by Strong Electrostatic Ion Cyclotron Turbulence, J. Geophys. Res., 85, 678, 1980.

13. Chang, T. and Coppi, B.: Lower Hybrid Accelertion and Ion Evolution in the Supraauroral Region, Geophys. Res. Lett., 18, 1253, 1981.

14. Hardy, D. A., W. J. Burke, and M. S. Gussenhoven: DMSP Optical and Electron Measurements in the Vicinity of Polar Cap Arcs, J. Geophys. Res., 87, 2413, 1982.

15. Burch, J. L., S. A. Fields, and R. A. Heelis: Polar Cap Electron Acceleration Regions, J. Geophys. Res., 84, 5863, 1979.

16. Burke, W. J., M. S. Gussenhoven, M. C. Kelley, D. A. Hardy, and F. J. Rich: Electric and Magnetic Field Characteristics of Discrete Arcs in the Polar Cap, J. Geophys. Res., 87, 2431, 1982.

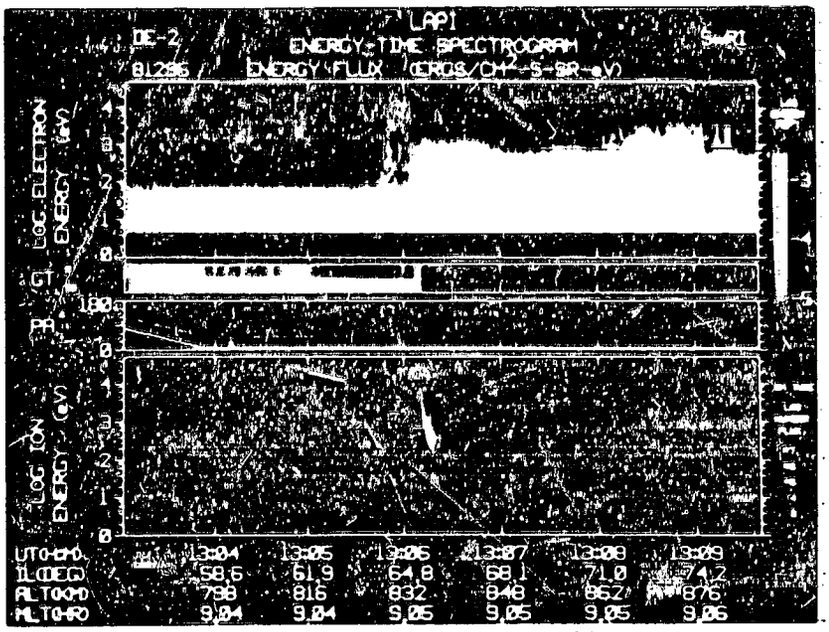

(a) 13:04 to 13:09 UT.

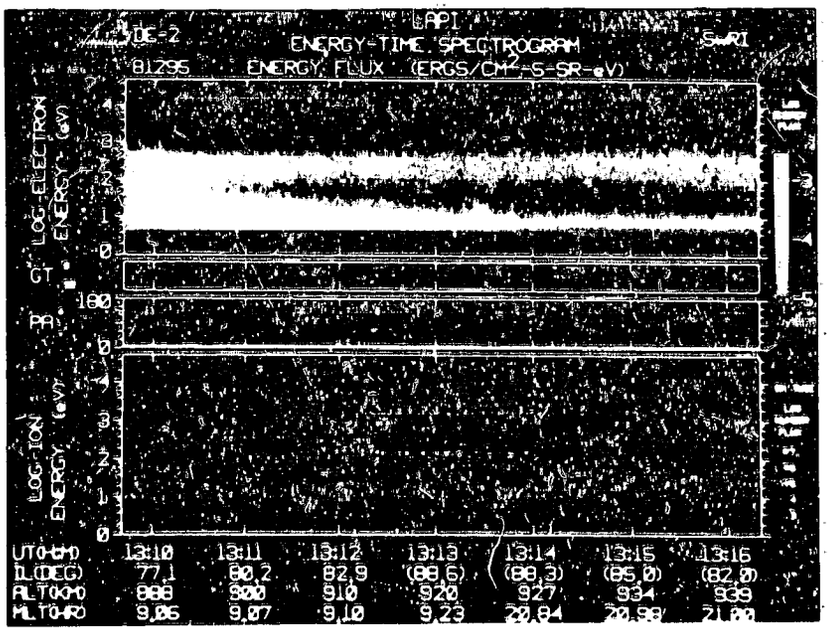

(b) 13:10 to 13:16 UT.

Figure 1. - LAPI energy-time spectrogram for DE-2, day 295 of 1981.

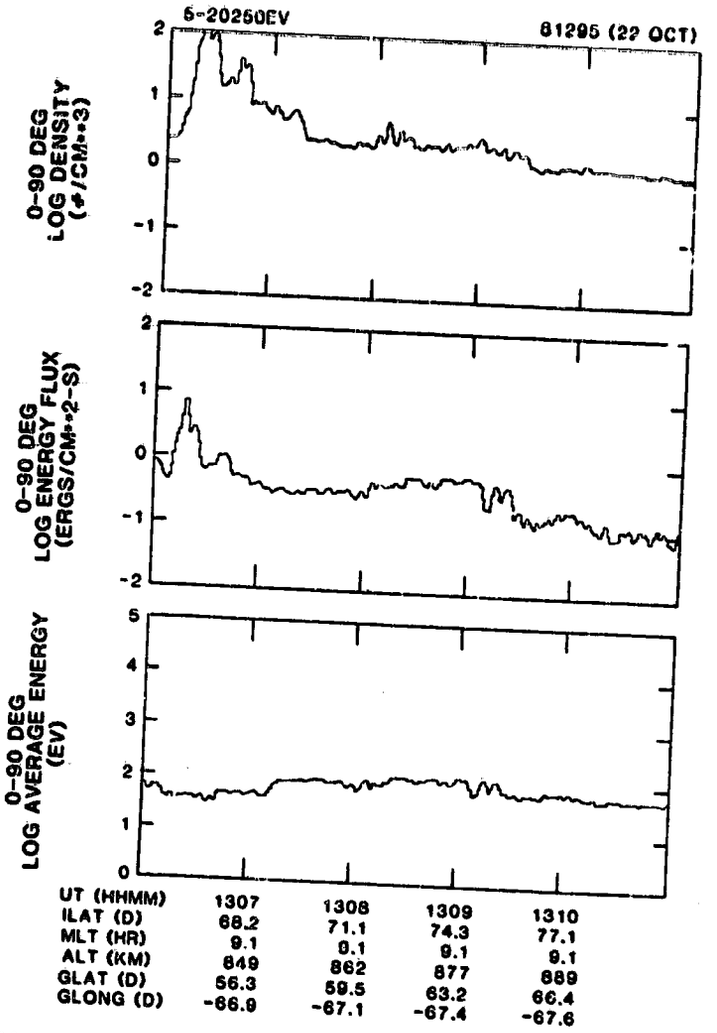

Figure 2. - DE-2 electrons, day 295 of 1981.

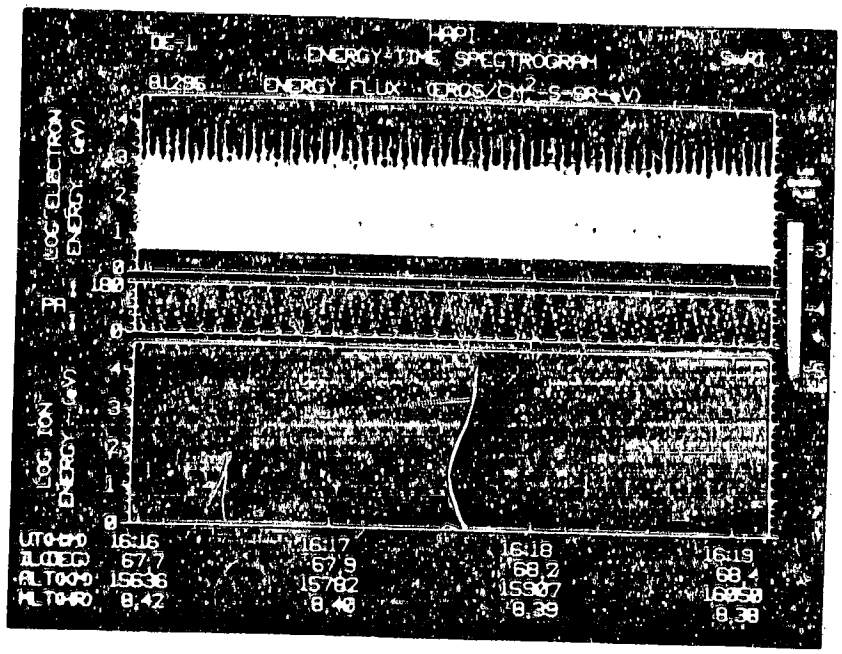

Figure 3. - HAPI energy-time spectrogram for DE-1, day 295 of 1981.

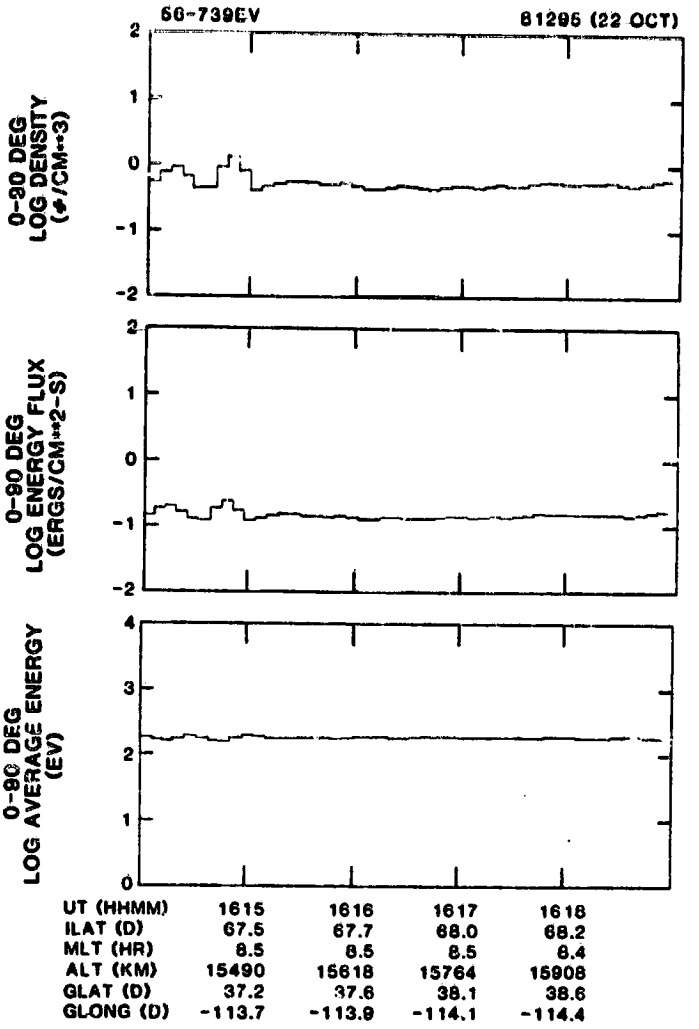

Figure 4. - DE-1 electrons, day 295 of 1981.

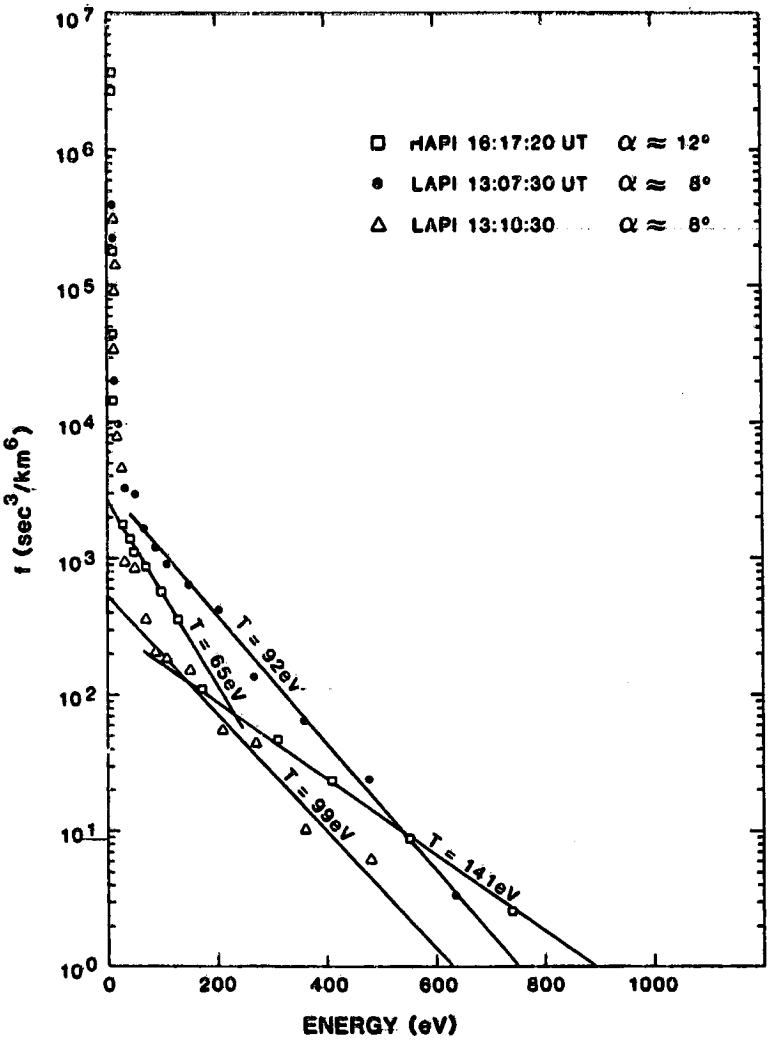

Figure 5. - Near-field-aligned electron populations.

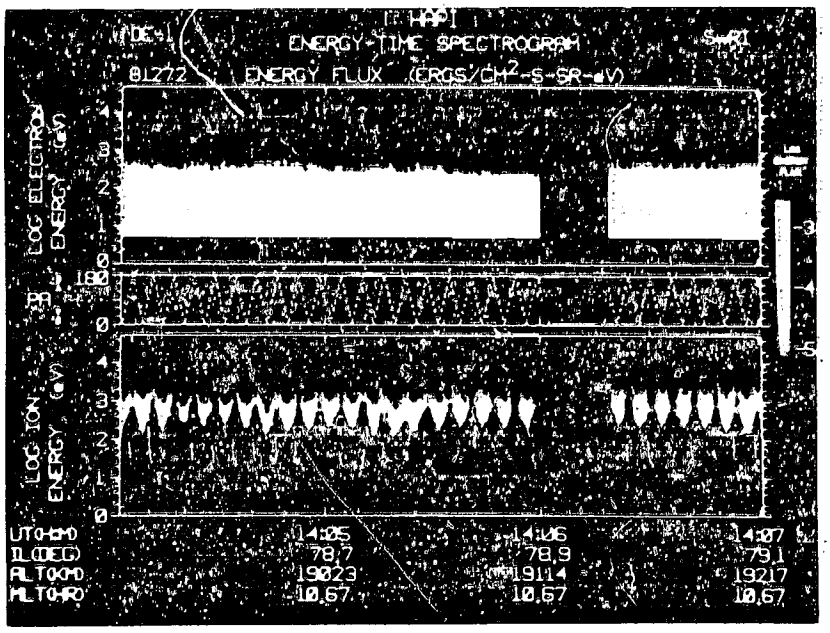

(a) 14:04 to 14:07 UT.

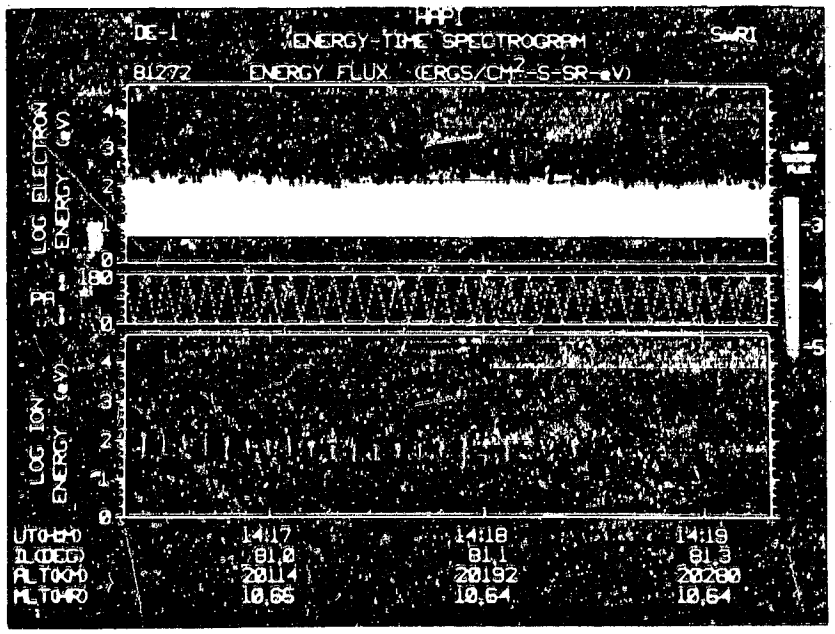

(b) 14:16 to 14:19 UT.

Figure 6. - HAPI energy-time spectrogram of DE-1, day 272 of 1981.

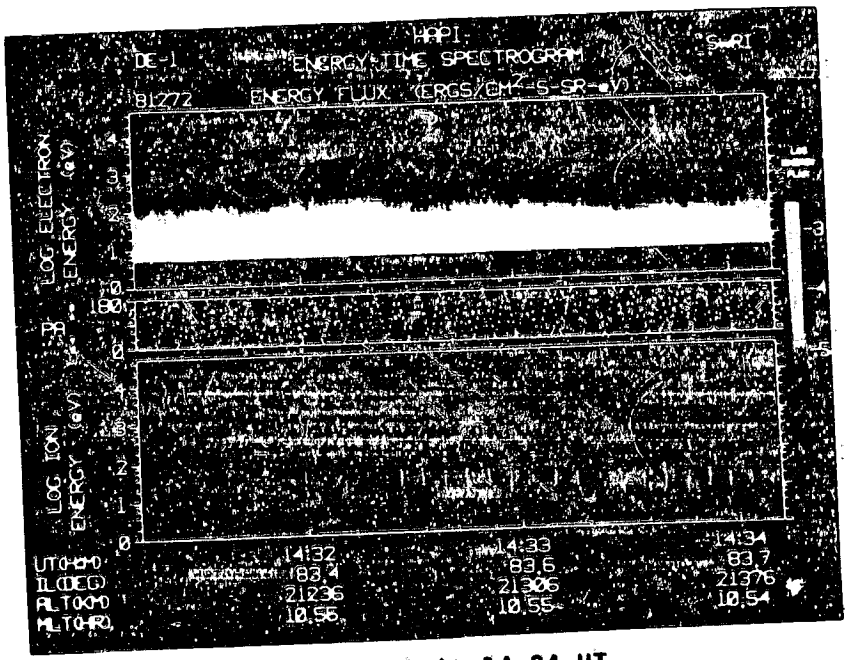

(c) 14:31 to 14:34 UT.

Figure 6. - Concluded.

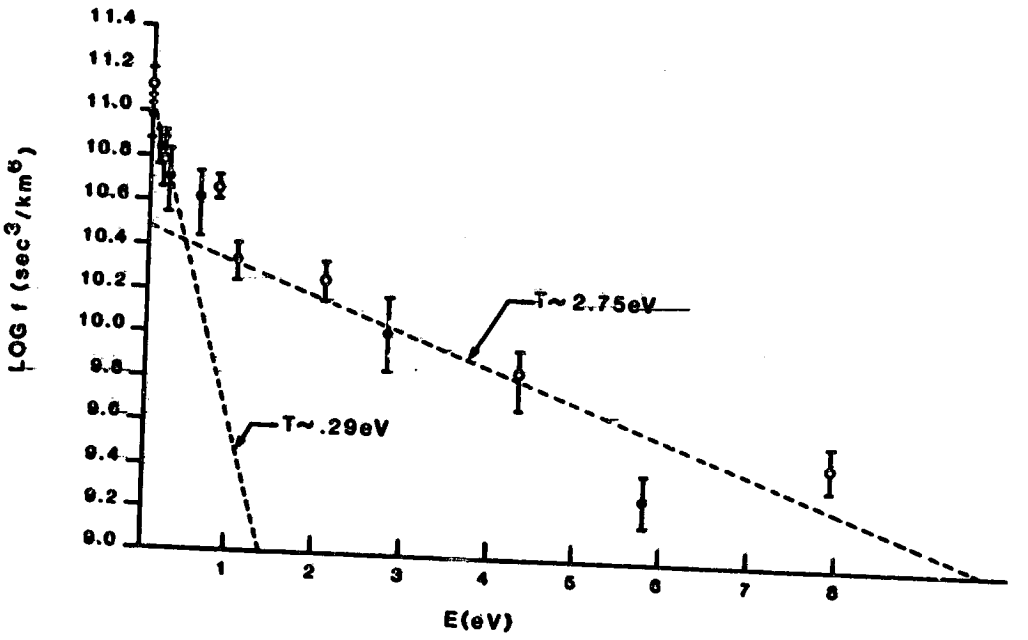

Figure 7. - HAPI velocity space spectrum.

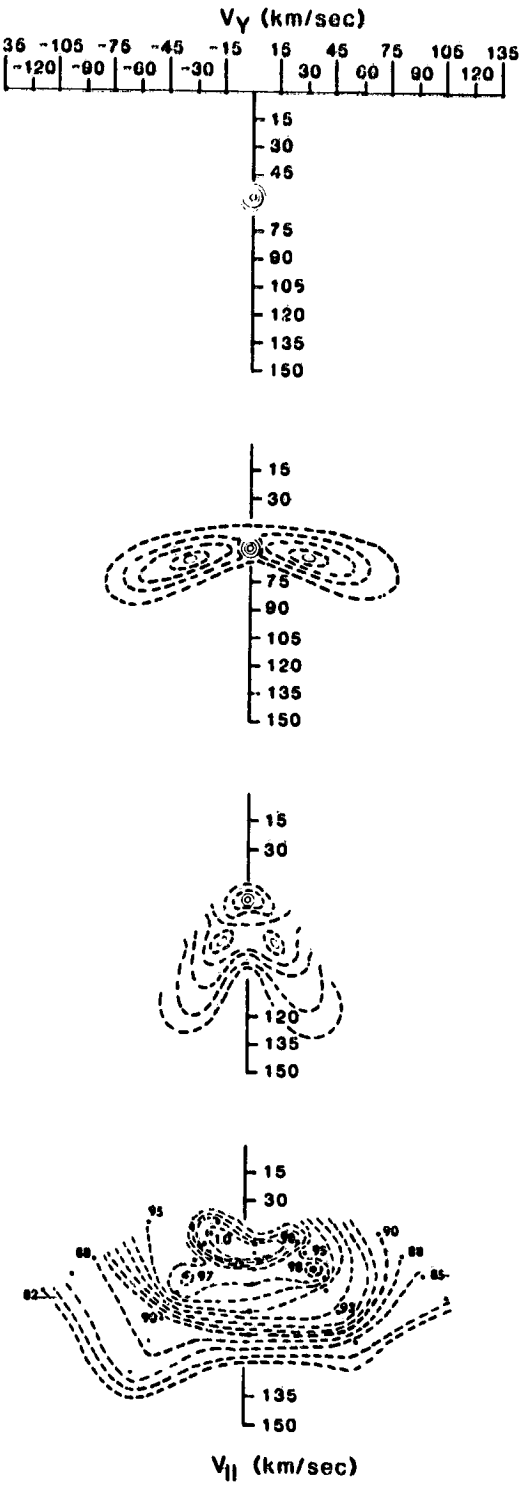

Figure 8. - Evolution of polar wind.

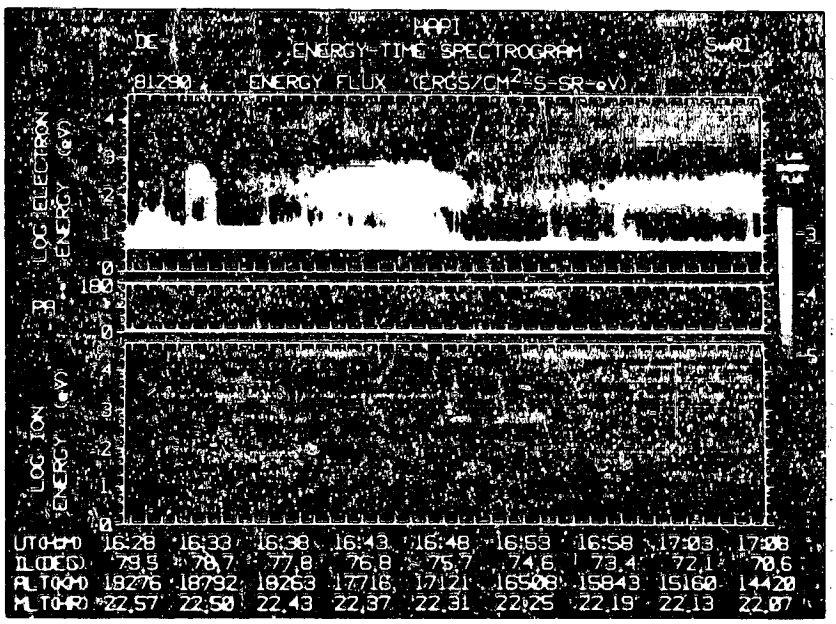

Figure 9. - HAPI energy-time spectrogram of DE-1, day 290 of 1981.

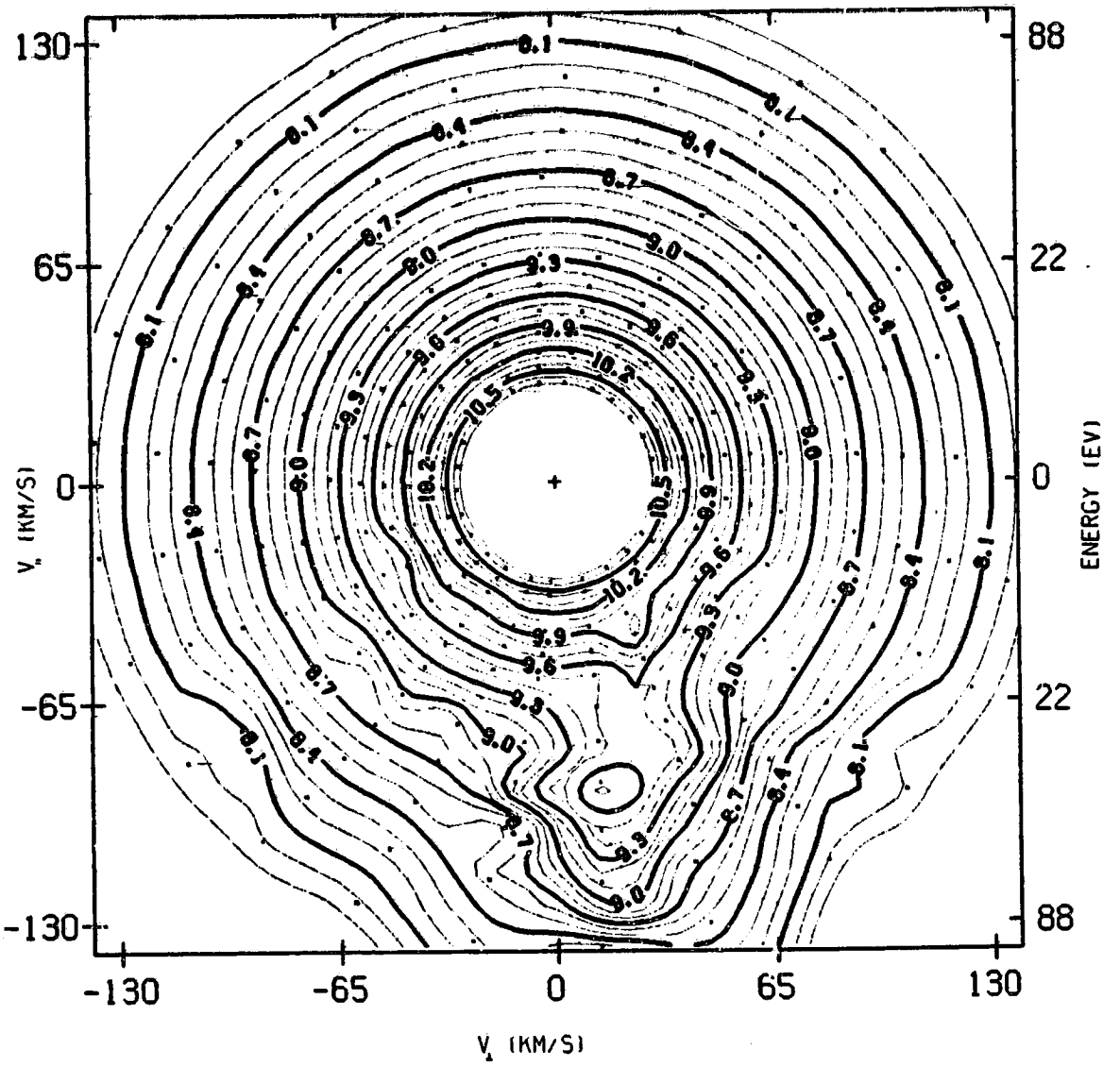

DISTRIBUTION CONTOURS LOG F (SEC³/KM⁶)

ILAT (D) 78.8	MIN EV	MAX EV	AV. EV.	AMPS/M²
MLT (HR) 22.6	6.	417.	4.17E+01	-1.47E-08
ALT (KM) 18819				
GLAT (D) 75.9				
GLONG (D) 66.3				

FLUX (/CM²S)	DEN (/CM³)	ERGS/CM²S
90 - 180	90 - 180	90 - 180
1.05E+07	1.27E+00	9.69E-04

VPAR (KM/S)	PC (MHOS)	HC (MHOS)
-7.23E+01	N/A	N/A

(a) Ions.

Figure 10. - HAPI contour plots for DE-1, day 290 of 1981, 16:32:45.1 to 16:32:57.1 UT.

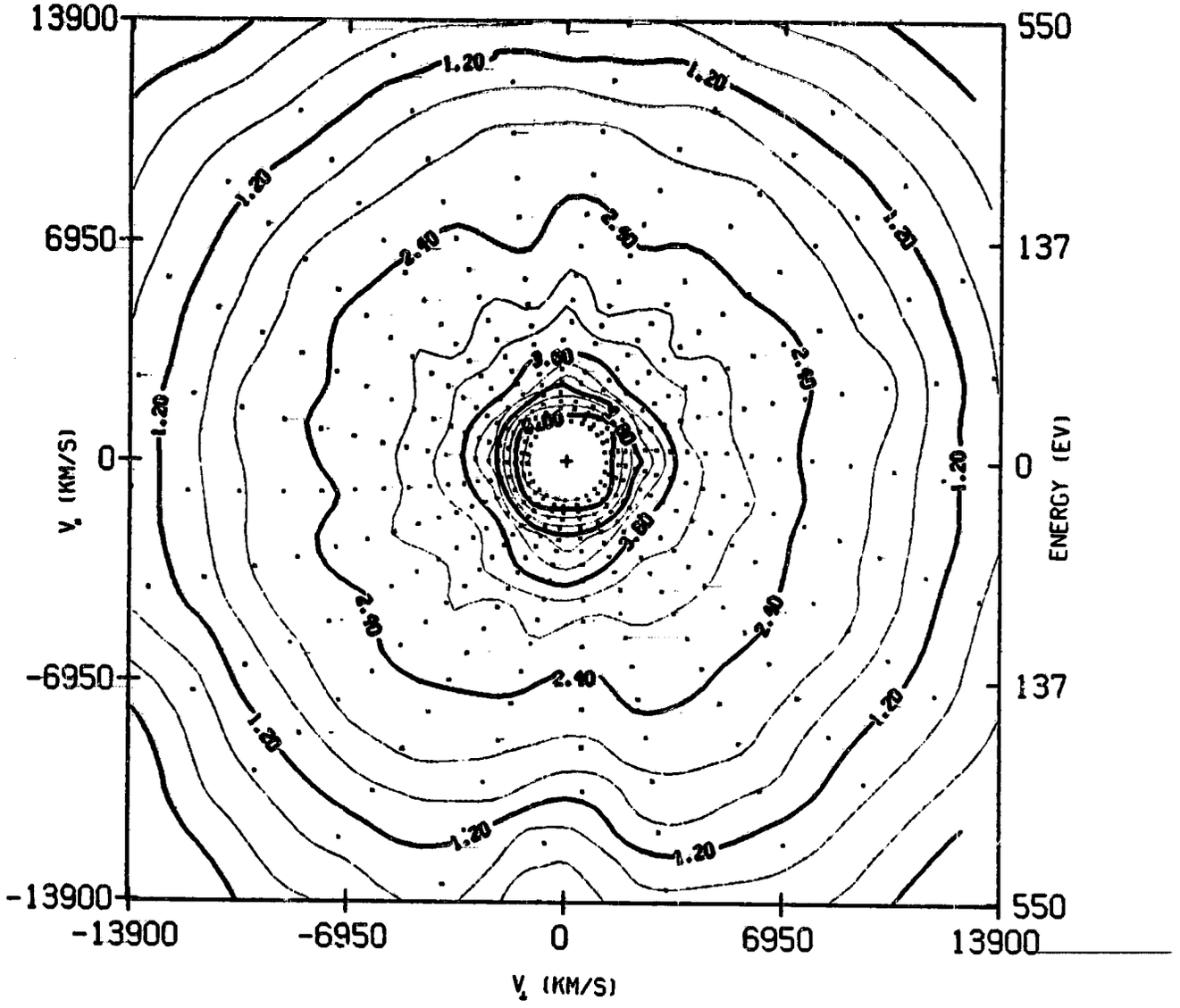

DISTRIBUTION CONTOURS LOG F (SEC³/KM⁶)

LAT (D)	78.8	MIN EV	MAX EV	AV. EV.	AMPS/M²
MLT (HR)	22.6	6.	739.	1.60E+01	-1.47E-07
ALT (KM)	18819				
GLAT (D)	75.9				
GLONG (D)	66.3				

FLUX (/CM²S)	DEN (/CM³)	ERGS/CM²S
0 - 90	0 - 90	0 - 90
4.02E+09	2.04E+01	2.04E-01

VPAR (KM/S)	PC (MHOS)	HC (MHOS)
-2.24E+01	N/A	N/A

(b) Electrons.

Figure 10. - Concluded.

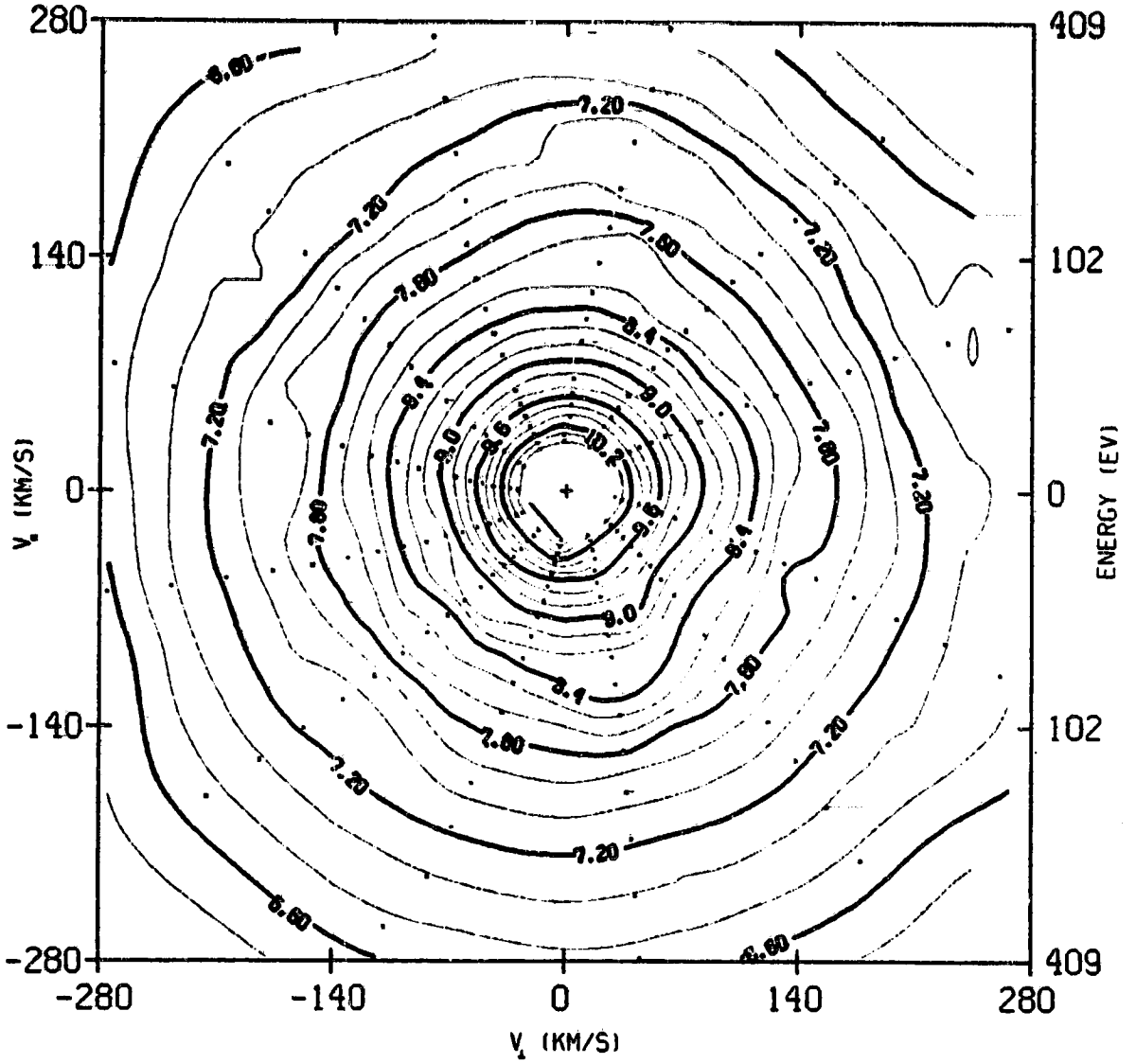

DISTRIBUTION CONTOURS LOG F (SEC³/KM⁶)

ILAT (D) 76.1	MIN EV	MAX EV	AV. EV.	AMPS/M²
MLT (HR) 22.4	6.	554.	2.91E+02	-3.77E-09
ALT (KM) 17313				
GLAT (D) 70.7				
GLONG (D) 69.0				

FLUX (/CM²S)	DEN (/CM³)	EAGS/CM²S
0 - 90	0 - 90	0 - 90
9.44E+06	4.17E-01	5.09E-03

VPAR (KM/S)	PC (MHOS)	HC (MHOS)
-1.32E+01	N/A	N/A

(a) Ions.

Figure 11. - HAPI contour plots for DE-1, day 290 of 1981, 16:46:30.0 to 16:46:35.7 UT.

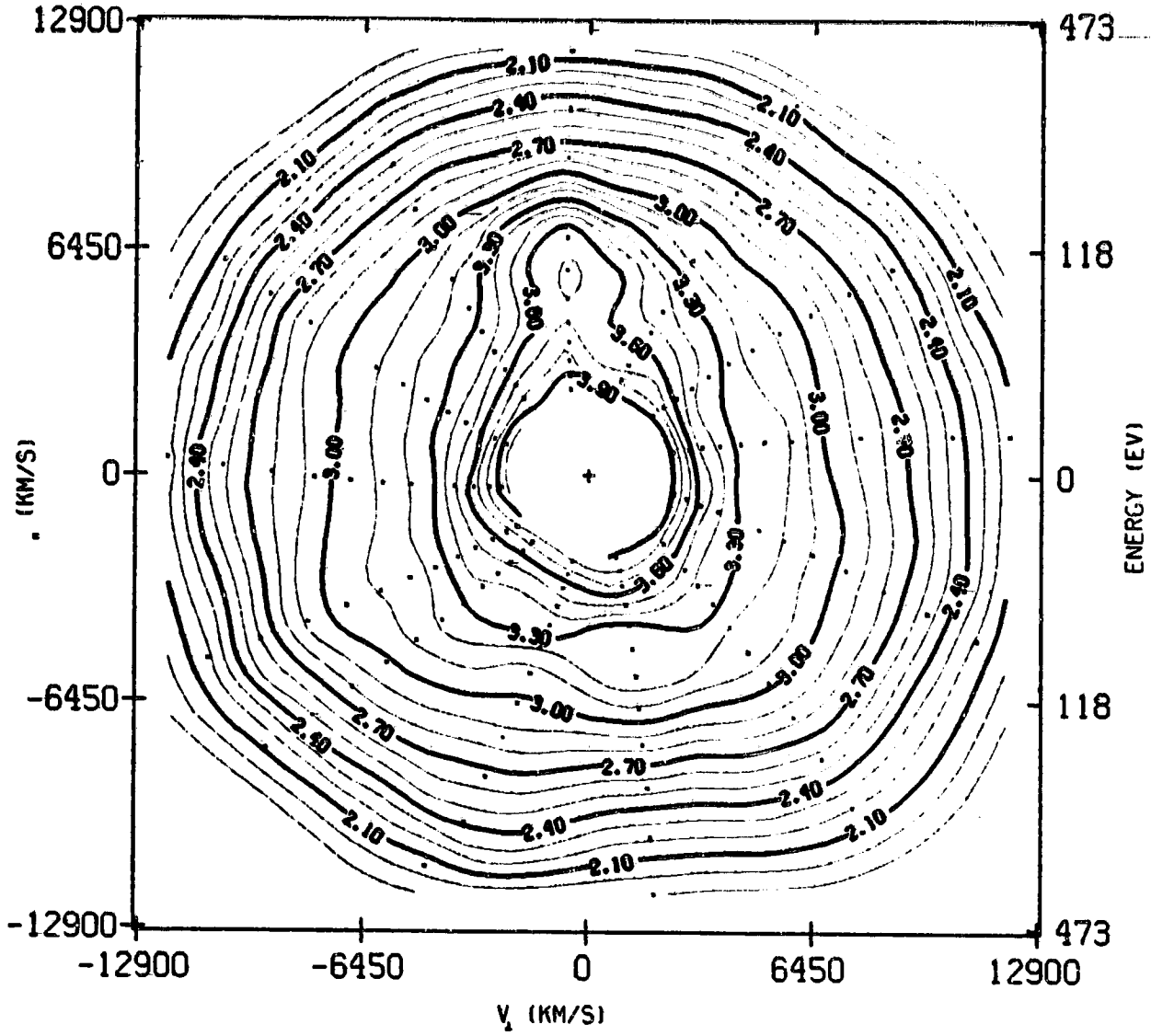

ILAT (D) 70.1			
MLT (HR) 22.4			
ALT (KM) 17297			
GLAT (D) 70.6			
GLONG (D) 63.0			
MIN_EV	MAX_EV	AV. EV.	AMPS/M²
10.	13206.	1.96E+02	6.61E-08
FLUX (/CM²S)		DEN (/CM³)	ERGS/CM²S
0 - 90		0 - 90	0 - 90
2.29E+09		9.03E+00	1.07E+00
VPAR (KM/S)		PC (MHOS)	HC (MHOS)
6.76E+01		2.069	2.908

(b) Electrons.

Figure 11. - Concluded.